Propofol reversibly attenuates short-range microstate ordering and 20 Hz microstate oscillations

Gesine Hermann
Christian-Albrechts University, University Hospital Schleswig Holstein
Inken Tödt
Christian-Albrechts University, University Hospital Schleswig-Holstein
Enzo Tagliazucchi
University of Buenos Aires
Inga Karin Todtenhaupt
Christian-Albrechts University, University Hospital Schleswig Holstein
Helmut Laufs
Christian-Albrechts University, University Hospital Schleswig Holstein
Frederic von Wegner (f.vonwegner@unsw.edu.au)
UNSW

Research Article

Keywords:

Posted Date: May 12th, 2023

DOI: https://doi.org/10.21203/rs.3.rs-2911395/v1

Additional Declarations: No competing interests reported.

Version of Record: A version of this preprint was published at Brain Topography on January 16th, 2024.
See the published version at https://doi.org/10.1007/s10548-023-01023-1.

Abstract

Microstate sequences summarize the changing voltage patterns measured by electroencephalography (EEG), using a clustering approach to reduce the high dimensionality of the underlying data. A common approach is to restrict the pattern matching step to local maxima of the global field power (GFP) and to interpolate the microstate fit in between. In this study, we investigate how the anesthetic propofol affects microstate sequence periodicity and predictability, and how these metrics are changed by interpolation.

We performed two frequency analyses on microstate sequences, one based on time-lagged mutual information, the other based on Fourier transform methodology, and quantified the effects of interpolation. Resting-state microstate sequences had a 20 Hz frequency peak related to dominant 10 Hz (alpha) rhythms, and the Fourier approach demonstrated that all five microstate classes followed this frequency. The 20 Hz periodicity was reversibly attenuated under moderate propofol sedation, as shown by mutual information and Fourier analysis. Characteristic microstate frequencies could only be observed in non-interpolated microstate sequences and were masked by smoothing effects of interpolation. Information-theoretic analysis revealed faster microstate dynamics and larger entropy rates under propofol, whereas Shannon entropy did not change significantly. In moderate sedation, active information storage decreased for non-interpolated sequences. Signatures of non-equilibrium dynamics were observed in non-interpolated sequences only and decreased in moderate sedation. All changes occurred while subjects were able to perform an auditory perception task.

In summary, we show that low-dose propofol reversibly increases the randomness of microstate sequences and attenuates microstate oscillations without correlation to cognitive task performance. Microstate dynamics between GFP peaks reflect physiological processes that are not accessible in interpolated sequences.

Introduction

EEG microstate analysis has become a common method to characterize EEG sequences, both in the resting state and in behavioral paradigms (Koenig et al. 2002; Khanna et al. 2015). The method generates chains of representative topographies enabling the reduction of the EEG signal to a one-dimensional string of categorical variables (microstate classes) whose content can provide insight into underlying brain processes. The ability to investigate microstate sequences with techniques from information theory and time series analysis (Lizier et al. 2012; von Wegner & Laufs 2018) has led to explorations of the temporal structure of sequences (von Wegner 2018; Tait et al. 2020; Zanesco et al. 2020; Artoni et al. 2022), as opposed to studies of individual states, their duration and precise topography. This focus is of particular interest for the study of resting state EEG due to the analogy between the sequence of microstates and sequences of brain states interpreted as the stream of consciousness (Deco et al. 2011; Michel & Koenig 2018; Artoni et al. 2022).

Conceivable ways of applying the method include many clinical questions. The initial development and use of the method were driven by research on neuropsychiatric conditions like schizophrenia, dementia, and depression, among others (Strik et al. 1995, 1997; Koenig et al. 1999; Lehmann et al. 2005; Kikuchi et al. 2007). Examining not only the duration and topographic properties of individual microstates, but also their temporal complexity enabled Tait et al. (2020) to differentiate between healthy controls and mild cognitive impairment. Members of our research group reported differences in the structure of sequences between physiological and pathological sleep patterns (Brodbeck et al. 2012, Kuhn et al. 2015). These were not only evident "macroscopically" during visual inspection of the EEG as traditionally used for sleep scoring (Kales & Rechtschaffen 1968; Iber et al. 2007), but also at the microstate level where microstate sequences in narcolepsy were fragmented compared to healthy controls (Kuhn et al. 2015). The diagnostic capabilities of microstate analysis in the field of neuropsychiatric diseases, especially those with reduced conscious alertness, are promising and offer opportunities for further methodological development and standardization (Bréchet & Michel 2022; Toplutaş et al. 2023).

Defining homogenous groups of subjects with disorders of consciousness can be difficult in clinical practice due to different aetiologies, comorbidities, age differences between groups, or diverse drug combinations. An alternative is to compare healthy subjects in wakefulness and under anesthesia. EEG microstate analysis during propofol sedation favors five microstate maps, compared to the commonly used four canonical resting state maps (Michel & Koenig 2018). Previous studies have reported changes in microstate duration in deep perioperative (Lapointe et al. 2023) and in light sedation stages (Shi et al. 2020; Artoni et al. 2022). Artoni et al. applied Lempel-Ziv compression to microstate sequences under propofol anesthesia and described sequence complexity as a function of depth of anesthesia (Artoni et al. 2022). Under mild to moderate propofol anesthesia, spatiotemporal EEG patterns were more diverse, as measured by an increased sequence complexity. Complexity decreased with deepening anesthesia, resulting in an inverse U-shaped dependence of complexity on anesthetic depth (Artoni et al. 2022). EEG and behavioral data from a study of mild to moderate sedation without loss of consciousness have been made publicly available and provide the basis of this report (Chennu et al. 2016). In that study, only 7/20 subjects presented impaired responsiveness to an auditory stimulus under moderate propofol sedation (target plasma concentration 1.2 µg/ml), and alpha frequency band phase connectivity before propofol injection predicted the behavioral effects (Chennu et al. 2016).

To date, only a small number of studies have investigated the characteristics of microstate sequences between different propofol sedation levels that would be clinically described as wakefulness. Shi et al. (2020) studied spectral EEG properties during the lifetime of individual microstates, and Artoni et al. (2022) investigated microstate sequence complexity, the latter study including light and deep sedation depths. The mapping of discrete pharmacologically induced changes and their quantitative description is of particular interest as they might have discriminatory power in detecting early stages of disorders associated with reduced conscious alertness. In this study, we test whether low propofol concentrations affect the frequency composition and information-theoretic predictability of EEG microstate sequences.

Once microstate sequences have been calculated by backfitting the microstate maps into the EEG time series, one can either work with the unaltered non-interpolated sequence (von Wegner et al. 2017, 2021), or a smoothing operation can be applied. A strong form of smoothing occurs when microstates are only fitted to GFP peak locations and all time points in between are assigned to the state at the closest GFP peak, a discrete version of interpolation (Michel & Koenig 2018; Schiller et al. 2019; Schumacher et al. 2019; Krylova et al. 2021). Intermediate smoothing intensities can be obtained by regularized filtering (Pascual-Marqui et al. 1995; Tomescu et al. 2014). In previous studies, we have found distinct time-periodic signatures in sequences that optimally represent the concurrent EEG topography at each time stamp, that is non-interpolated microstate sequences (von Wegner et al. 2021). Each interpolation choice brings certain advantages and disadvantages, and the methods are rarely compared directly. We will therefore compare non-interpolated and GFP peak-interpolated sequences obtained from the propofol dataset (Chennu et al. 2016).

Our first aim is to investigate putative changes in microstate periodicity under propofol in both, non-interpolated and GFP peak-interpolated sequences. We hypothesize that temporal smoothing will attenuate the periodicity observed in non-interpolated sequences. Based on the findings of Chennu et al. (2016), who reported reduced phase-coupling in the alpha frequency band under propofol, we hypothesize that microstate sequences will decorrelate faster, corresponding to a higher entropy rate, and that this might also affect their periodic ordering. This hypothesis is based on the findings that the alpha frequency band contributes most to resting-state microstates (Milz et al. 2017), and that fixed phase relationships between electrodes are necessary to generate stable topographic maps, i.e. microstates (Koenig & Valdés-Sosa 2018). To quantify the temporal order of microstates, we apply information-theoretic measures on non-interpolated and interpolated sequences. Additionally, we test effects of propofol on the asymmetry of microstate transition matrices (von Wegner et al. 2017). Asymmetry indicates time-irreversibility of microstate sequences and departure from equilibrium dynamics. A loss of time-irreversibility has recently been discussed as a marker of transitions to unconsciousness, based on studies in non-human primates (de la Fuente et al. 2023).

Methods

Experimental data

The dataset published by Chennu et al. (2016) contains EEG recordings from n = 20 healthy subjects (9 male) with a mean age of 30.85 years (SD = 10.98 years). All recordings were acquired in an eyes-closed condition. Each participant underwent four EEG recordings - one at baseline, during mild sedation (target propofol plasma concentration (PPC) 0.6 µg/ml), moderate sedation (target PPC 1.2 µg/ml) and at recovery, each lasting 7 minutes. The published datasets are partitioned into 10 second artifact-free segments. We removed those subjects from the dataset that were classified as ‘drowsy’ in (Chennu et al. 2016) as we found signatures of N1 and N2 sleep stages in some of their baseline condition recordings. This resulted in a subset of 13 subjects for further analysis.

The dataset also contains results from a behavioral task performed during each of the four sedation levels. Subjects were asked to distinguish two auditory stimuli (n = 40, 2 blocks, mean inter-stimulus interval 3 sec) with a key press. Hit rates and reaction times were recorded. See (Chennu et al. 2016) for further details.

EEG signal processing

All data sets were recorded with a 128 channel EEG setup, sampled at 250 Hz, using the Net Amps 300 amplifier (Electrical Geodesics Inc., Eugene, Oregon, USA). Data were re-referenced to an average reference as recommended for microstate analysis (Murray et al. 2008). A total of 91 EEG channels were retained after artifact rejection.

Band-pass filtering used zero-phase, 6-th order Butterworth coefficients with a transfer function slope of 24 dB/octave and 1–30 Hz passband for microstate analysis. EEG topographies were interpolated and projected on a 128 × 128 grid using cubic Clough-Tocher interpolation for visual display (von Wegner & Laufs 2018). The EEG spectral density was computed on the time-course of the first principal component (PC-1) of each EEG dataset using Welch's algorithm with a Hann window (256 samples wide, 50% overlap) implemented in the SciPy library (Virtanen et al. 2020), as previously reported (von Wegner et al. 2017, 2021).

Microstate algorithm

Subject-wise microstates were computed with the modified K-means algorithm (Pascual-Marqui et al. 1995; Murray et al. 2008), using EEG voltage vectors at GFP peaks as input. We used K = 5 clusters following Shi et al. (2020) who analyzed the same dataset and used the Krzanowski-Lai criterion. Group-wise microstates were computed by a full permutation procedure (Koenig et al. 2002) with 20 random initializations. Grand mean microstate maps were obtained from clustering across the four conditions (sedation levels). Microstate sequences were obtained by either (i) competitive back-fitting of the five grand mean maps to each time step and no further processing (non-interpolated sequences), or, (ii) back-fitting to GFP peak locations and assignment of all other time steps to the map at the closest GFP peak (interpolated sequences).

Microstate sequence analysis

Frequency Analysis

We applied two methods to identify the spectral properties of microstate sequences. The first method used time-lagged mutual information (autoinformation function, AIF), introduced in (von Wegner et al. 2017) and the code published in (von Wegner & Laufs 2018).

The second method is based on classical Fourier transform spectral analysis and yields one frequency spectrum per microstate class. To apply a discrete Fourier transform to the categorical microstate variables (A, B, C, …), we transformed each microstate sequence into five different numerical sequences

as follows. For a sequence of microstate labels $L\left(n\right)$ (discrete time $n = 0,1,\ldots$) and microstate label $l \in \{A, B, C, D, F\}$, we computed a transform that we call the characteristic microstate sequence $x_l\left(n\right)$ as $x_l\left(n\right) = 1$ if $L\left(n\right) = l$ and $x_l\left(n\right) = 0$ else. For instance, the label sequence $L\left(n\right) = (A, A, B, A, C, B, D)$ yields the characteristic sequences $x_A\left(n\right) = (1,1,0,1,0,0,0)$, $x_B\left(n\right) = (0,0,1,0,0,1,0)$, and so on. For each characteristic sequence we computed the power spectral density with Welch's algorithm and Hann window (256 samples, 50% overlap).

Information-theoretic Analysis

Microstate sequences were further characterized by their Shannon entropy (h_0), entropy rate (h_1), and active information storage (AIS). Entropy calculations were carried out as detailed in (von Wegner et al. 2017; von Wegner & Laufs 2018). AIS has been applied to discrete dynamical systems before (Lizier et al. 2012; Wibral et al. 2014) but not to EEG microstate sequences. In terms of probabilities, the entropy rate is derived from the conditional distribution $P\left(X_{n+1}|X_n, \ldots, X_{n-k+1}\right)$ of the next microstate label X_{n+1}, given knowledge about the past k microstate labels $X_n, \ldots, X_{n-k+1}$, whereas AIS refers to the shared information $I\left(X_{n+1}; X_n, \ldots, X_{n-k+1}\right)$ between the next state and the k past states. Since the total entropy of microstate sequences can change between conditions, entropy rate and AIS are not necessarily anti-correlated across conditions. Eq. (1) illustrates the mathematical relationship between the three measures (Lizier et al. 2012). The left-hand side is the Shannon entropy (h_0) of the next microstate (time point $n + 1$) which can be expressed as the sum of the entropy rate (h_1, first right-hand side term) and active information storage (AIS, second right-hand side term). Entropy rate and AIS are written in the form of their finite history length (k) estimates which were used in computations.

$$H\left(X_{n+1}\right) = H\left(X_{n+1}|X_n, \ldots, X_{n-k+1}\right) + I\left(X_{n+1}; X_n, \ldots, X_{n-k+1}\right) \quad (1)$$

All calculations were implemented as detailed in (von Wegner 2018; von Wegner et al. 2018) with a history length of k = 5 samples.

The microstate transition probability matrix $T_{ij} = P\left(X_{n+1} = S_j|X_n = S_i\right)$ for the microstate classes $S = \{A, B, C, D, F\}$ was quantified by its relaxation time (von Wegner et al. 2017) to obtain a measure of the overall rate of change of microstate dynamics. A shorter relaxation time indicates faster decorrelation of the sequence.

Temporal irreversibility

Temporal irreversibility was assessed by testing the symmetry of the microstate transition probability matrix (von Wegner et al. 2017). Rejection of the null hypothesis (symmetry) at α = 0.01 was taken as evidence that the microstate sequence had an 'arrow of time' (Kim et al. 2018; de la Fuente et al. 2023). For each subject we determined the fraction of time-irreversible microstate segments and averaged this fraction across subjects in each condition.

Statistical Analysis

All analyses were implemented in the Python 3 programming language (Van Rossum & Drake 2009). Statistical analyses were computed with the statsmodels toolbox (Seabold & Perktold 2010).

Results

Microstate maps

Figure 1 shows the microstate maps obtained for each sedation stage and the resulting grand mean maps (last row) that were used for further analysis. The microstate maps A - F in Fig. 1 show good agreement with recent studies of propofol sedation but also with maps reported in other experimental conditions (Custo et al. 2017; Shi et al. 2020; Zanesco et al. 2020; Artoni et al. 2022; Hao et al. 2022). Map similarity measured by the absolute value of the spatial cross-correlation coefficient revealed minor differences between the sedation levels. The largest difference from baseline was observed for map F under moderate sedation (Table 1). Our map F under moderate sedation was similar to map D in Shi et al. (2020) and Zhang et al. (2021). This difference did not affect further analyses which were based on the grand mean maps (GM in Fig. 1). The global explained variance for the grand mean maps (GEV = 68.7%) was in the range reported for resting-state conditions.

Table 1
Spatial correlation between maps displays the largest difference between baseline and moderate sedation. Maps A, B, C, D and F at baseline were compared to mild sedation, moderate sedation and the recovery stage.

	map A	map B	map C	map D	map F	average per stage
baseline vs. mild sedation	0.994	0.986	0.998	0.994	0.994	0.993
baseline vs. moderate sedation	0.988	0.979	0.957	0.940	0.657	0.904
baseline vs. recovery	0.901	0.926	0.966	0.988	0.989	0.954

Microstate frequency analysis

Spectral properties of microstate sequences were measured in the time and frequency domain. In the time domain, we applied time-lagged mutual information (autoinformation function, AIF) to measure two-point autocorrelations for discrete time lags (0-400 ms).

Figure 2 shows the AIF (mean and 95% confidence intervals) for non-interpolated microstate sequences on the left and for GFP-peak interpolated microstate sequences on the right. Sedation levels are listed from top to bottom (a - d) as indicated by the annotations. These were the main observations:

i) Microstate sequences occurred periodically with a minimum time lag of 50 ms at a) baseline, b) mild sedation and during d) recovery. This periodicity was attenuated during c) moderate sedation.

ii) The effects described in i) were not observed for interpolated sequences (right column). Interpolated microstate sequences did not show periodic microstate sequence features in any sedation level.

Results from the methodologically independent Fourier transform-based method are illustrated in Fig. 3. This method allowed frequency domain analysis of individual microstate classes. The power spectral densities (PSD) of characteristic microstate sequences for microstate classes A to F (different line styles) showed no qualitative differences between the microstate classes. The spectral properties of the underlying EEG at the sensor level were summarized by the PSD of the first principal component of the EEG data set (blue, mean PSD and 95% confidence interval). EEG spectra are identical for non-interpolated (left) and interpolated (right) microstate sequences and demonstrate dominant alpha frequencies around 10 Hz in a) baseline, b) mild sedation, and d) recovery. For c) moderate propofol sedation, alpha frequency band power was clearly reduced. Non-interpolated microstate spectra (left column) displayed dominant frequencies at twice the alpha frequency (20 Hz) whenever the EEG alpha peak was observable (a-d), and was strongly attenuated for all microstate classes under c) moderate propofol sedation. The PSDs of interpolated microstate sequences decayed monotonously (right column), and did not display characteristic spectral peaks across the four sedation levels (a-d).

Microstate sequence parameters

The statistics of the microstate sequence parameters relaxation time (τ), Shannon entropy (h_0), entropy rate (h_1), and active information storage (AIS) are illustrated in Fig. 4 for non-interpolated sequences (a, b) and GFP peak-interpolated sequences (c, d). Row a) and c) show their statistics (mean, standard deviation, n = 13) for each sedation level and row b) and d) show their dependence on the propofol plasma concentration (PPC).

Relaxation time and entropy rate analysis of a) non-interpolated and c) interpolated sequences demonstrated a shorter relaxation time and a larger entropy rate in moderate sedation, compared to baseline and recovery. Active information storage was reduced in moderate sedation for non-interpolated sequences and correlated negatively with PPC. Correlation analysis with PPC confirmed these relationships for b) non-interpolated sequences. In c) interpolated sequences, significant correlations were observed for τ, h_0 and h_1. Where significant, the correlation coefficients for non-interpolated and interpolated sequences had the same sign. It should be noted that the absolute values of microstate sequence parameters depend on the pre-processing strategy (non-interpolated vs. interpolated).

Temporal Irreversibility

Temporal irreversibility of microstate sequences is analyzed in Fig. 5. For each subject and each EEG segment (10 sec), symmetry of the transition probability matrix was tested statistically and the fraction of rejected null hypotheses was recorded for each subject. In Fig. 5, statistics (mean, standard deviation)

across subjects (n = 13) are shown for a) non-interpolated and b) interpolated microstate sequences. Statistical analysis revealed a reduced fraction of asymmetric (time-irreversible) transition matrices in moderate sedation, compared to baseline and recovery. Note the different y-axis scaling in b) as we found almost no evidence for asymmetric transition matrices in interpolated sequences. There were no significant differences between sedation levels in b).

Correlation between microstate parameters and behavior

Figure 6 summarizes the results for the behavioral markers reaction time (a, c) and percentage of correct answers (b, d) for non-interpolated (a, b) and interpolated (c, d) sequences. Spearman correlation coefficients were computed between the microstate sequence parameters (relaxation time, Shannon entropy, entropy rate, AIS) and the behavioral markers pooled across sedation levels. Sedation levels are indicated by different markers (legend in the upper right corner). This resulted in 16 correlation analyses which were Bonferroni corrected. No significant correlations were found.

Discussion

To investigate whether and how propofol sedation alters EEG microstate sequences, we analyzed sequence properties in both non-interpolated and GFP-peak interpolated data from a publicly available dataset. The main results of our study were:

- Propofol had marked effects on microstate dynamical properties at moderate sedation levels (propofol plasma concentration 1.2 µg/ml).
- Propofol sedation reversibly attenuated 20 Hz oscillatory patterns that were present in microstate sequences at baseline. This affected all microstate classes and was related to a decrease in 10 Hz EEG power at the sensor level.
- Propofol led to faster microstate dynamics (shorter relaxation time), reduced sequence predictability (higher entropy rate, lower active information storage), and dynamics indicative of a brain state closer to equilibrium dynamics.
- The aforementioned changes were mostly observed in non-interpolated microstate sequences. Sequence interpolation between GFP peaks obscured spectral changes and features indicative of non-equilibrium dynamics.
- All propofol-induced changes represented low sedation levels without loss of consciousness and at least partially preserved task performance.

Propofol-induced changes in microstate periodicity

Microstate sequence periodicity is one of several quantitative features that demonstrate temporal ordering principles of spontaneous brain state dynamics and is observable in healthy subjects at rest (von Wegner et al. 2017) and during cognitive processing (Jia et al. 2021). While the baseline is characterized by 20 Hz microstate oscillations (twice the alpha frequency, von Wegner et al. 2021),

cognitive task execution leads to a shift towards higher frequencies as beta frequencies become more prominent (Jia et al. 2021). We investigated sequence periodicity with two independent methods in the time and frequency domain, respectively, and related microstate frequency spectra to those of the underlying EEG at the sensor level. The main effect of propofol at moderate plasma concentrations (target 1.2 µg/ml) was an attenuation of periodic features at 20 Hz, or at time lags of 50 ms and multiples thereof (Fig. 2, Fig. 3) in non-interpolated microstate sequences. The newly introduced Fourier transform-based method proved that this effect occurred for all five microstate classes. Both methods complement each other in that AIF includes all microstate classes, whereas the Fourier transform-based method yields one spectrum per class. AIF has the advantage of being robust against variations in the chosen number of microstates (supplementary material in (von Wegner et al. 2017)). We confirmed the robustness of AIF and PSD analyses on the propofol dataset when using K = 4 microstates (data not shown).

In Fig. 4, residual alpha power at the EEG sensor level was observed in the frequency spectrum of the EEG's first principal component in agreement with Chennu et al. (2016) and Shi et al. (2020). An even stronger reduction of occipital alpha power is expected during deeper propofol sedation with concomitant loss of consciousness, where delta and beta activity are known to dominate the EEG (Purdon et al. 2013). Several groups have demonstrated increased frontocentral alpha amplitudes under deeper propofol sedation rather than a pure decrease in occipital alpha activity (Akeju et al. 2014; Kallionpää et al. 2020). For the data used in this study, Chennu et al. (2016) showed a preserved posterior dominant alpha power topography even under moderate sedation.

Our results show that microstate periodicities could not be mapped in GFP peak-interpolated data. This supported our initial hypothesis that the inevitable smoothing effects of interpolation would affect temporal sequence features observable at higher temporal resolution. The reversible modulation of periodicities by propofol suggests that microstate dynamics between GFP peaks convey physiologically relevant information, although these topographies display lower GFP values (Zanesco et al. 2020) and are sometimes assumed to contain mostly noise.

Shi et al. (2020) chose a related, but fundamentally different approach by analyzing power spectra at the EEG sensor level restricted to the lifetime of GFP-peak interpolated microstates of a given class (marginal spectrum). Both approaches reveal reduced alpha frequency band power, yet the results in Shi et al. (2020) do not provide information about the periodic occurrence of microstates themselves. The marginal EEG spectra in Shi et al. (2020) are compatible with both the presence and absence of periodic microstates. The key determinant is the extent of phase-locking between electrodes (Koenig & Valdés-Sosa 2018). Uncoupled, phase-independent alpha oscillators could still produce alpha frequency peaks at individual sensors, and thus in the marginal spectra, but would destroy the periodic recurrence of individual microstates. Our results demonstrate that periodicity is one aspect of temporal microstate ordering that is present in the baseline but is lost at relatively low propofol concentrations and even before impairment of cognitive task performance occurs.

In summary, non-interpolated microstate sequences contain frequency information that can be pharmacologically modulated and is not accessible in interpolated sequences.

Microstate sequence predictability and information storage

Apart from periodicity, we evaluated non-interpolated and interpolated microstate sequences regarding their relaxation time (τ), Shannon entropy (h_0), entropy rate (h_1), and active information storage (AIS).

The relaxation time of a sequence is calculated from the transition probability matrix and therefore informs about single time step transitions ($n \rightarrow n+1$). An advantage over the full matrix representation is that τ quantifies the transition probabilities across all microstates. More formally, τ describes how fast the microstate generating process approaches equilibrium if perturbed. We found reduced relaxation times under moderate propofol sedation in non-interpolated and interpolated sequences (Fig. 4). Interpolated sequences have larger absolute τ values as interpolation introduces longer state durations and therefore a slower approach to equilibrium. Assuming that microstate sequences are not completely deterministic but contain some inherent stochasticity, a shorter relaxation time suggests a reduced predictability of future states from past values, as the correlation with past states is lost over a smaller number of time steps. In terms of brain state dynamics, this indicates a lower coherence of brain states over time, or in other words, that past brain states exert less influence on which network will be activated in the next step (Jia et al. 2021). The limitation of the relaxation time approach is the short time window considered and that it describes linear system properties only. Markov surrogate data of microstate sequences are constructed from the same transition matrix as the actual EEG-derived sequence and therefore have identical relaxation times, but they do not model periodic microstate properties (von Wegner et al. 2017). Relaxation time is thus a useful descriptor of global time scale changes between experimental conditions but cannot be expected to capture all aspects of temporal order.

Entropy rates were computed for a history length of five samples, which was limited by the length of EEG segments (10 sec). Longer histories require more samples to reliably estimate the joint entropies from which the entropy rate was calculated. Although there were no significant differences between sedation levels for total Shannon entropy, entropy rates increased in deeper sedation and correlated positively with the propofol plasma concentration (Fig. 4). There are two interpretations of entropy rates, first as a measure of time series complexity in the sense of randomness, the other as a measure of sequence predictability. Our findings indicate that microstate sequences are less ordered and closer to a random sequence at moderate propofol concentrations. Technically, given a sequence of brain activations, these states are less useful in predicting which activation pattern the brain will generate next. In Jia et al. (2021), this effect was interpreted in terms of putative cognitive control networks which appear to be less active, or less effective, during the execution of creative tasks, allowing for more degrees of freedom in choosing the next functional network to become active. In the context of propofol, we hypothesize that these control mechanisms are pharmacologically constrained and less capable to direct the flow of network activity. With regard to Kolmogorov complexity, microstate sequences under propofol are more complex compared to baseline. Our results can therefore be translated to the findings that Artoni et al.

(2022) reported for Lempel-Ziv complexity, which is another measure of Kolmogorov complexity. The two approaches, based on two different datasets, agree in describing an increased sequence complexity at low propofol concentrations which might be related to a transient hyperexcitable brain state (Ching & Brown 2014).

AIS measures whether correlations between past states can be used to predict the next brain state. The concept is closely related to entropy rate and indeed, for a constant total (Shannon) entropy h_0, the sum of entropy rate (h_1) and AIS equals h_0. As we could not predict whether h_0 would change under propofol, we evaluated all three quantities. Statistical analysis revealed no significant changes in h_0 between sedation levels but the linear correlation between propofol concentration and Shannon entropy of interpolated sequences was positive. Active information storage only showed changes for non-interpolated sequences, and these were concordant with the entropy rate changes discussed in the previous paragraph. With increasing entropy rate at deeper sedation levels, lower AIS values demonstrate that correlations with past microstates contribute significantly less to future states.

A reduced fraction of asymmetric transition matrices, i.e., time-irreversible microstate dynamics, was observed under moderate sedation for non-interpolated sequences (Fig. 5). Loss of temporal directionality can be interpreted as a dynamic state closer to equilibrium and was observed during the transition to unconscious states in non-human primates in (Sanz Perl et al. 2021) and (de la Fuente et al. 2023). Sanz Perl et al. (2021) used an approach similar to ours but based on electrocorticography data. Data were discretized and the asymmetry of the transition probability matrix was used to measure how far brain activity was from thermodynamic equilibrium. The authors found that different states of reduced consciousness were associated with brain states closer to equilibrium, including sleep and several anesthetic drugs (Sanz Perl et al. 2021). The underlying concept is that living systems, and especially the brain as an information processing subsystem, are not expected to be operative close to thermodynamic equilibrium. We addressed the question of non-equilibrium dynamics under propofol which has not been answered for human EEG microstate sequences. In our earlier study 14/20 subjects showed evidence of non-equilibrium microstate dynamics in relaxed wakefulness (von Wegner et al. 2017). We now found that moderate propofol sedation was associated with microstate dynamics closer to equilibrium, in accordance with Sanz Perl et al. (2021) and de la Fuente et al. (2023). Our data shows that the shift towards equilibrium dynamics in humans occurs even before consciousness and cognitive performance are markedly affected. The lower fraction of non-equilibrium sequences at baseline (resting-state) compared to our earlier study is probably explained by shorter EEG segments in the underlying dataset (10 sec). The null hypothesis of the statistical test is symmetry, which is more likely to be accepted for smaller sample sizes, i.e., shorter sequences (lower test power). Test results for interpolated microstate sequences make clear that interpolation produced a drastic shift towards symmetry as non-equilibrium dynamics were almost absent at baseline. Given evidence from other studies, we believe that the shift towards equilibrium dynamics observed in interpolated sequences is an artificial effect that obscures potentially relevant features of true brain state dynamics.

It remains an open question whether hysteresis effects as described in (Kim et al. 2018) for ketamine and sevoflurane anesthesia can be found in EEG microstate data under propofol. Our statistical analysis between the sedation depths labeled by (Chennu et al. 2016) revealed no significant differences between baseline and recovery, that is induction of and emergence from anesthesia. This could also be due to the comparatively light sedation level. Microstate analysis of continuous EEG recordings during induction and emergence might help to answer this question.

Sedation with maintained awareness

All results describe changes in healthy subjects without loss of consciousness. We excluded a subgroup of subjects (n = 7) from the published dataset. Chennu et al. (2016) described a subgroup of n = 7 subjects with significantly reduced stimulus perception rates in this dataset. Upon visual inspection of the non-interpolated EEG segments, we found EEG features of light sleep in their baseline condition. We therefore excluded this subgroup from our analyses while they were included in other studies (Chennu et al. 2016; Shi et al. 2020). The remaining subgroup (n = 13) was assumed to be awake at all sedation depths as their perceptual hit rates were above 80% for all but one subject even under moderate propofol sedation. Thus, stages of quantitatively altered consciousness in a clinical sense were not reached. Nevertheless, mild propofol sedation induced significant changes that could be quantified with spectral and information-theoretic measures. In analogy to the results by Artoni et al. (2022), it would also be interesting to track the measures introduced in this study in deeper sedation stages with loss of consciousness. As an outlook, the same methods could be employed to assess pathologically reduced states of consciousness.

In summary, our study provides new insights into the pharmacological modifiability of microstate syntax principles, in particular their periodic properties and short-range predictability. Propofol reversibly attenuates microstate periodicity and moves microstate transitions closer to equilibrium dynamics, but these effects can be obscured by microstate sequence interpolation.

Declarations

Acknowledgements

This work was funded by the German Research Foundation (DFG), project number 440536202.

The authors thank the researchers Chennu et al. (2016) for the publication of their dataset.

Conflict of interest

The authors declare that they have no conflict of interest.

References

1. Akeju, O., Pavone, K. J., Westover, M. B., Vazquez, R., Prerau, M. J., Harrell, P. G., Hartnack, K. E., Rhee, J., Sampson, A. L., Habeeb, K., Gao, L., Pierce, E. T., Walsh, J. L., Brown, E. N., & Purdon, P. L. (2014). A Comparison of Propofol- and Dexmedetomidine-induced Electroencephalogram Dynamics Using Spectral and Coherence Analysis. *Anesthesiology*, *121*(5), 978–989. https://doi.org/10.1097/ALN.0000000000000419
2. Artoni, F., Maillard, J., Britz, J., Seeber, M., Lysakowski, C., Bréchet, L., Tramèr, M. R., & Michel, C. M. (2022). EEG microstate dynamics indicate a U-shaped path to propofol-induced loss of consciousness. *NeuroImage*, *256*. https://doi.org/10.1016/j.neuroimage.2022.119156
3. Bréchet, L., & Michel, C. M. (2022). EEG Microstates in Altered States of Consciousness. *Frontiers in Psychology*, *13*, 1549. https://doi.org/10.3389/FPSYG.2022.856697/BIBTEX
4. Brodbeck, V., Kuhn, A., von Wegner, F., Morzelewski, A., Tagliazucchi, E., Borisov, S., Michel, C. M., & Laufs, H. (2012). EEG microstates of wakefulness and NREM sleep. *NeuroImage*, *62*(3), 2129–2139. https://doi.org/10.1016/j.neuroimage.2012.05.060
5. Chennu, S., O'Connor, S., Adapa, R., Menon, D. K., & Bekinschtein, T. A. (2016). Brain Connectivity Dissociates Responsiveness from Drug Exposure during Propofol-Induced Transitions of Consciousness. *PLoS Computational Biology*, *12*(1), 1–17. https://doi.org/10.1371/journal.pcbi.1004669
6. Ching, S., & Brown, E. N. (2014). Modeling the dynamical effects of anesthesia on brain circuits. *Current Opinion in Neurobiology*, *25*, 116–122. https://doi.org/10.1016/j.conb.2013.12.011
7. Custo, A., Van De Ville, D., Wells, W. M., Tomescu, M. I., Brunet, D., & Michel, C. M. (2017). Electroencephalographic Resting-State Networks: Source Localization of Microstates. *Brain Connectivity*, *7*(10), 671–682. https://doi.org/10.1089/brain.2016.0476
8. de la Fuente, L. A., Zamberlan, F., Bocaccio, H., Kringelbach, M., Deco, G., Perl, Y. S., Pallavicini, C., & Tagliazucchi, E. (2023). Temporal irreversibility of neural dynamics as a signature of consciousness. *Cerebral Cortex*, *33*(5), 1856–1865. https://doi.org/10.1093/cercor/bhac177
9. Deco, G., Jirsa, V. K., & McIntosh, A. R. (2011). Emerging concepts for the dynamical organization of resting-state activity in the brain. In *Nature Reviews Neuroscience* (Vol. 12, Issue 1, pp. 43–56). https://doi.org/10.1038/nrn2961
10. Hao, Z., Zhai, X., Cheng, D., Pan, Y., & Dou, W. (2022). EEG Microstate-Specific Functional Connectivity and Stroke-Related Alterations in Brain Dynamics. *Frontiers in Neuroscience*, *16*. https://doi.org/10.3389/fnins.2022.848737
11. Iber, C., Ancoli-Israel, S., Chesson, A., & Quan, S. F. (2007). *The AASM Manual for the Scoring of Sleep and Associated Events: Rules, Terminology and Technical Specifications* (1st ed.). American Academy of Sleep Medicine.
12. Jia, W., von Wegner, F., Zhao, M., & Zeng, Y. (2021). Network oscillations imply the highest cognitive workload and lowest cognitive control during idea generation in open-ended creation tasks. *Scientific Reports*, *11*(1). https://doi.org/10.1038/s41598-021-03577-1

13. Kales, A., & Rechtschaffen, A. (1968). A manual of standardized terminology, techniques and scoring system for sleep stages of human subjects. In *National Institutes of Health publication* (Vol. 204). U. S. National Institute of Neurological Diseases and Blindness, Neurological Information Network.
14. Kallionpää, R. E., Valli, K., Scheinin, A., Långsjö, J., Maksimow, A., Vahlberg, T., Revonsuo, A., Scheinin, H., Mashour, G. A., & Li, D. (2020). Alpha band frontal connectivity is a state-specific electroencephalographic correlate of unresponsiveness during exposure to dexmedetomidine and propofol. *British Journal of Anaesthesia*, *125*(4), 518–528. https://doi.org/10.1016/j.bja.2020.05.068
15. Khanna, A., Pascual-Leone, A., Michel, C. M., & Farzan, F. (2015). Microstates in resting-state EEG: Current status and future directions. *Neuroscience & Biobehavioral Reviews*, *49*, 105–113. https://doi.org/10.1016/j.neubiorev.2014.12.010
16. Kikuchi, M., Koenig, T., Wada, Y., Higashima, M., Koshino, Y., Strik, W., & Dierks, T. (2007). Native EEG and treatment effects in neuroleptic-naïve schizophrenic patients: Time and frequency domain approaches. *Schizophrenia Research*, *97*(1–3), 163–172. https://doi.org/10.1016/j.schres.2007.07.012
17. Kim, H., Moon, J. Y., Mashour, G. A., & Lee, U. C. (2018). Mechanisms of hysteresis in human brain networks during transitions of consciousness and unconsciousness: Theoretical principles and empirical evidence. *PLoS Computational Biology*, *14*(8). https://doi.org/10.1371/JOURNAL.PCBI.1006424
18. Koenig, T., Lehmann, D., Merlo, M. C. G., Kochi, K., Hell, D., & Koukkou, M. (1999). A deviant EEG brain microstate in acute, neuroleptic-naive schizophrenics at rest. *European Archives of Psychiatry and Clinical Neuroscience*, *249*(4), 205–211. https://doi.org/10.1007/s004060050088
19. Koenig, T., Prichep, L., Lehmann, D., Sosa, P. V., Braeker, E., Kleinlogel, H., Isenhart, R., & John, E. R. (2002). Millisecond by Millisecond, Year by Year: Normative EEG Microstates and Developmental Stages. *NeuroImage*, *16*, 41–48. https://doi.org/10.1006/nimg.2002.1070
20. Koenig, T., & Valdés-Sosa, P. A. (2018). Results Obtained by Combining Different Estimators of EEG Connectivity Become Uninterpretable If the Underlying Models Are Incompatible. *Https://Home.Liebertpub.Com/Brain*, *8*(2), 57–59. https://doi.org/10.1089/BRAIN.2017.0555
21. Krylova, M., Alizadeh, S., Izyurov, I., Teckentrup, V., Chang, C., van der Meer, J., Erb, M., Kroemer, N., Koenig, T., Walter, M., & Jamalabadi, H. (2021). Evidence for modulation of EEG microstate sequence by vigilance level. *NeuroImage*, *224*, 117393. https://doi.org/10.1016/J.NEUROIMAGE.2020.117393
22. Kuhn, A., Brodbeck, V., Tagliazucchi, E., Morzelewski, A., von Wegner, F., & Laufs, H. (2015). Narcoleptic Patients Show Fragmented EEG-Microstructure During Early NREM Sleep. *Brain Topography*, *28*(4), 619–635. https://doi.org/10.1007/s10548-014-0387-1
23. Lapointe, A. P., Li, D., Hudetz, A. G., & Vlisides, P. E. (2023). Microstate analyses as an indicator of anesthesia-induced unconsciousness. *Clinical Neurophysiology*, *147*, 81–87. https://doi.org/10.1016/j.clinph.2023.01.007

24. Lehmann, D., Faber, P. L., Galderisi, S., Herrmann, W. M., Kinoshita, T., Koukkou, M., Mucci, A., Pascual-Marqui, R. D., Saito, N., Wackermann, J., Winterer, G., & Koenig, T. (2005). EEG microstate duration and syntax in acute, medication-naïve, first-episode schizophrenia: A multi-center study. *Psychiatry Research - Neuroimaging*, *138*(2), 141–156. https://doi.org/10.1016/j.pscychresns.2004.05.007
25. Lennox, M. (1946). Effects of sedative drugs on the electroencephalogram. *American Journal of Psychiatry*, *102*(6), 799–804. https://doi.org/10.1176/ajp.102.6.799
26. Lizier, J. T., Prokopenko, M., & Zomaya, A. Y. (2012). Local measures of information storage in complex distributed computation. *Information Sciences*, *208*, 39–54. https://doi.org/10.1016/j.ins.2012.04.016
27. Michel, C. M., & Koenig, T. (2018). EEG microstates as a tool for studying the temporal dynamics of whole-brain neuronal networks: A review. *NeuroImage*, *180*(December 2017), 577–593. https://doi.org/10.1016/j.neuroimage.2017.11.062
28. Milz, P., Pascual-Marqui, R. D., Achermann, P., Kochi, K., & Faber, P. L. (2017). The EEG microstate topography is predominantly determined by intracortical sources in the alpha band. *NeuroImage*, *162*, 353–361. https://doi.org/10.1016/J.NEUROIMAGE.2017.08.058
29. Murray, M. M., Brunet, D., & Michel, C. M. (2008). Topographic ERP analyses: A step-by-step tutorial review. In *Brain Topography* (Vol. 20, Issue 4, pp. 249–264). https://doi.org/10.1007/s10548-008-0054-5
30. Pascual-Marqui, R. D., Michel, C. M., & Lehmann, D. (1995). Segmentation of brain electrical activity into microstates: model estimation and validation. *IEEE Transactions on Biomedical Engineering*, *42*(7), 658–665. https://doi.org/10.1109/10.391164
31. Purdon, P. L., Pierce, E. T., Mukamel, E. A., Prerau, M. J., Walsh, J. L., Wong, K. F. K., Salazar-Gomez, A. F., Harrell, P. G., Sampson, A. L., Cimenser, A., Ching, S., Kopell, N. J., Tavares-Stoeckel, C., Habeeb, K., Merhar, R., & Brown, E. N. (2013). Electroencephalogram signatures of loss and recovery of consciousness from propofol. *Proceedings of the National Academy of Sciences of the United States of America*, *110*(12). https://doi.org/10.1073/pnas.1221180110
32. Sanz Perl, Y., Bocaccio, H., Pallavicini, C., Pérez-Ipiña, I., Laureys, S., Laufs, H., Kringelbach, M., Deco, G., & Tagliazucchi, E. (2021). Nonequilibrium brain dynamics as a signature of consciousness. *Physical Review E*, *104*(1), 014411. https://doi.org/10.1103/PHYSREVE.104.014411/FIGURES/5/MEDIUM
33. Schiller, B., Koenig, T., & Heinrichs, M. (2019). Oxytocin modulates the temporal dynamics of resting EEG networks. *Scientific Reports 2019 9:1*, *9*(1), 1–9. https://doi.org/10.1038/s41598-019-49636-6
34. Schumacher, J., Peraza, L. R., Firbank, M., Thomas, A. J., Kaiser, M., Gallagher, P., O'Brien, J. T., Blamire, A. M., & Taylor, J. P. (2019). Dysfunctional brain dynamics and their origin in Lewy body dementia. *Brain*, *142*(6), 1767–1782. https://doi.org/10.1093/BRAIN/AWZ069
35. Seabold, S., & Perktold, J. (2010). statsmodels: Econometric and statistical modeling with python. In *9th Python in Science Conference*.

36. Shi, W., Li, Y., Liu, Z., Li, J., Wang, Q., Yan, X., & Wang, G. (2020). Non-Canonical Microstate Becomes Salient in High Density EEG during Propofol-Induced Altered States of Consciousness. *International Journal of Neural Systems*, *30*(2). https://doi.org/10.1142/S0129065720500057
37. Strik, W. K., Chiaramonti, R., Muscas, G. C., Paganini, M., Mueller, T. J., Fallgatter, A. J., Versari, A., & Zappoli, R. (1997). Decreased EEG microstate duration and anteriorisation of the brain electrical fields in mild and moderate dementia of the Alzheimer type. *Psychiatry Research: Neuroimaging*, *75*(3), 183–191. https://doi.org/10.1016/S0925-4927(97)00054-1
38. Strik, W. K., Dierks, T., Becker, T., & Lehmann, D. (1995). Larger topographical variance and decreased duration of brain electric microstates in depression. *Journal of Neural Transmission*, *99*(1–3), 213–222. https://doi.org/10.1007/BF01271480
39. Tait, L., Tamagnini, F., Stothart, G., Barvas, E., Monaldini, C., Frusciante, R., Volpini, M., Guttmann, S., Coulthard, E., Brown, J. T., Kazanina, N., & Goodfellow, M. (2020). EEG microstate complexity for aiding early diagnosis of Alzheimer's disease. *Scientific Reports*, *10*(1). https://doi.org/10.1038/s41598-020-74790-7
40. Tomescu, M. I., Rihs, T. A., Becker, R., Britz, J., Custo, A., Grouiller, F., Schneider, M., Debbané, M., Eliez, S., & Michel, C. M. (2014). Deviant dynamics of EEG resting state pattern in 22q11.2 deletion syndrome adolescents: A vulnerability marker of schizophrenia? *Schizophrenia Research*, *157*(1–3), 175–181. https://doi.org/10.1016/J.SCHRES.2014.05.036
41. Toplutaş, E., Aydın, F., & Hanoğlu, L. (2023). EEG Microstate Analysis in Patients with Disorders of Consciousness and Its Clinical Significance. *Brain Topography*, *1*, 1–11. https://doi.org/10.1007/S10548-023-00939-Y/FIGURES/5
42. Van Rossum, G., & Drake, F. L. (2009). *Python 3 Reference Manual*. CreateSpace.
43. Virtanen, P., Gommers, R., Oliphant, T. E., Haberland, M., Reddy, T., Cournapeau, D., Burovski, E., Peterson, P., Weckesser, W., Bright, J., van der Walt, S. J., Brett, M., Wilson, J., Millman, K. J., Mayorov, N., Nelson, A. R. J., Jones, E., Kern, R., Larson, E., … Vázquez-Baeza, Y. (2020). SciPy 1.0: fundamental algorithms for scientific computing in Python. *Nature Methods*, *17*(3), 261–272. https://doi.org/10.1038/s41592-019-0686-2
44. Von Wegner, F. (2018). Partial autoinformation to characterize symbolic sequences. *Frontiers in Physiology*, *9*(OCT), 1–14. https://doi.org/10.3389/fphys.2018.01382
45. von Wegner, F., Bauer, S., Rosenow, F., Triesch, J., & Laufs, H. (2021). EEG microstate periodicity explained by rotating phase patterns of resting-state alpha oscillations. *NeuroImage*, *224*. https://doi.org/10.1016/j.neuroimage.2020.117372
46. von Wegner, F., Knaut, P., & Laufs, H. (2018). EEG microstate sequences from different clustering algorithms are information-theoretically invariant. *Frontiers in Computational Neuroscience*, *12*(August), 1–14. https://doi.org/10.3389/fncom.2018.00070
47. von Wegner, F., & Laufs, H. (2018). Information-theoretical analysis of EEG microstate sequences in python. *Frontiers in Neuroinformatics*, *12*(June), 1–10. https://doi.org/10.3389/fninf.2018.00030

48. von Wegner, F., Tagliazucchi, E., & Laufs, H. (2017). Information-theoretical analysis of resting state EEG microstate sequences - non-Markovianity, non-stationarity and periodicities. In *NeuroImage* (Vol. 158). Elsevier Inc. https://doi.org/10.1016/j.neuroimage.2017.06.062
49. Wibral, M., Lizier, J. T., Vögler, S., Priesemann, V., & Galuske, R. (2014). Local active information storage as a tool to understand distributed neural information processing. *Frontiers in Neuroinformatics*, *8*. https://doi.org/10.3389/fninf.2014.00001
50. Zanesco, A. P., King, B. G., Skwara, A. C., & Saron, C. D. (2020). Within and between-person correlates of the temporal dynamics of resting EEG microstates. *NeuroImage*, *211*. https://doi.org/10.1016/j.neuroimage.2020.116631
51. Zhang, K., Shi, W., Wang, C., Li, Y., Liu, Z., Liu, T., Li, J., Yan, X., Wang, Q., Cao, Z., & Wang, G. (2021). Reliability of EEG microstate analysis at different electrode densities during propofol-induced transitions of brain states. *NeuroImage*, *231*, 117861. https://doi.org/10.1016/J.NEUROIMAGE.2021.117861

Figures

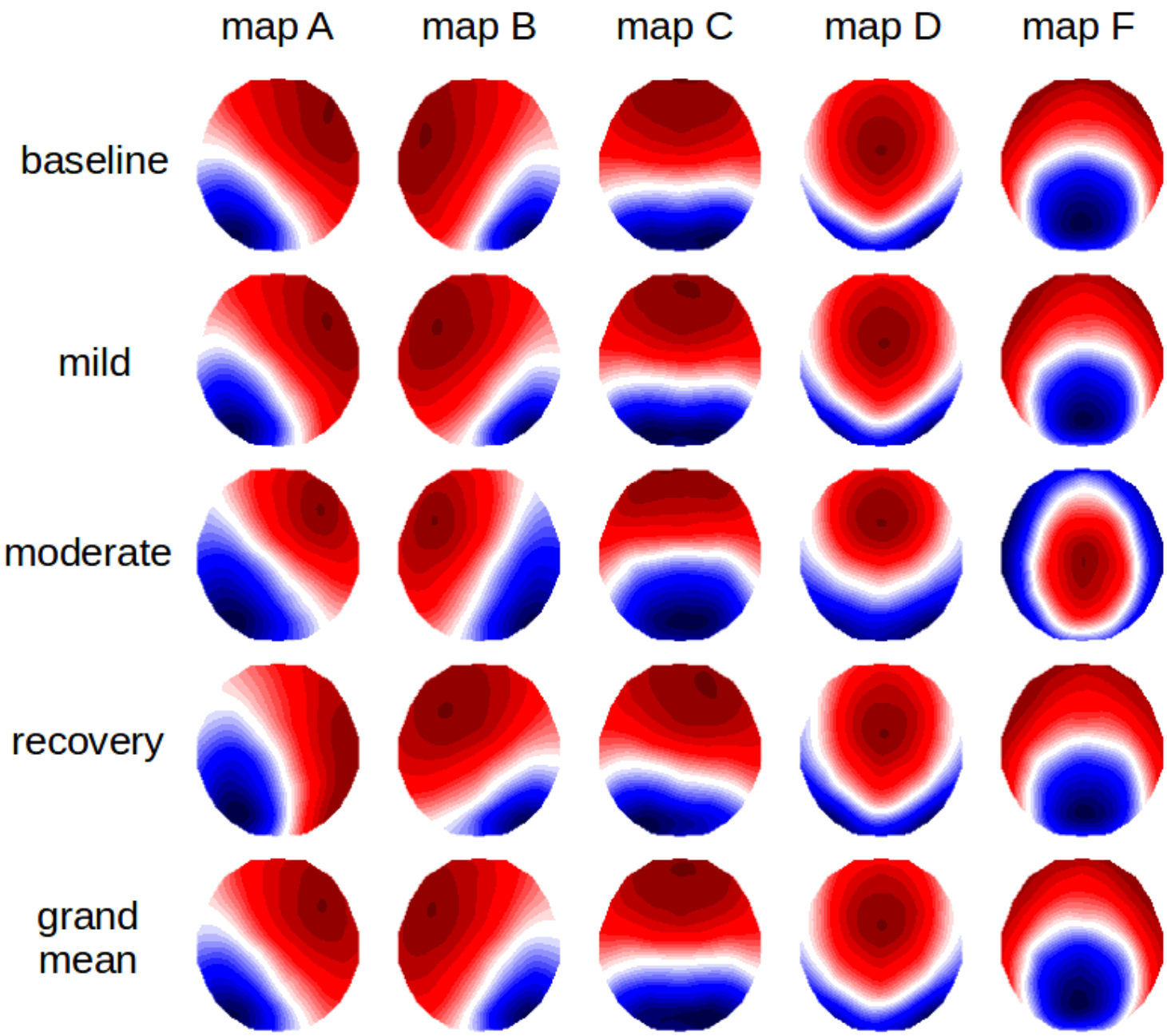

Figure 1

Microstate maps. *Map topographies are shown for each sedation level (baseline, mild sedation, moderate sedation, recovery) and the grand mean (GM) from the modified K-means algorithm. Map labeling follows Custo et al. (2017).*

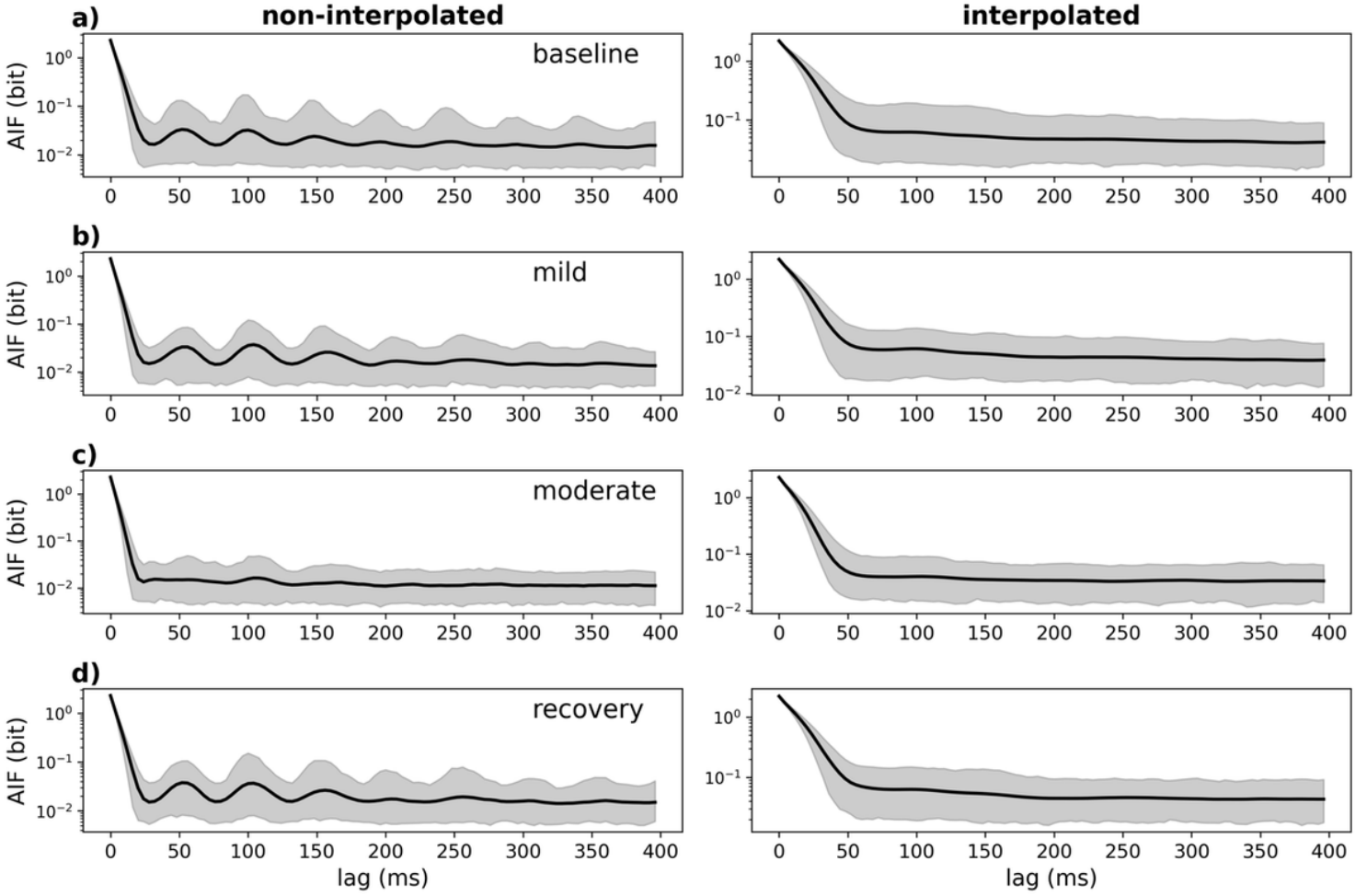

Figure 2

Microstate periodicity at multiples of approximately 50 ms (20 Hz) in non-interpolated sequences is attenuated under moderate propofol sedation. *Autoinformation functions (AIF) for the sedation levels a) baseline, b) mild sedation, c) moderate sedation, and d) recovery. The left column shows results for non-interpolated microstate sequences, the right column for GFP-peak interpolated microstate sequences.*

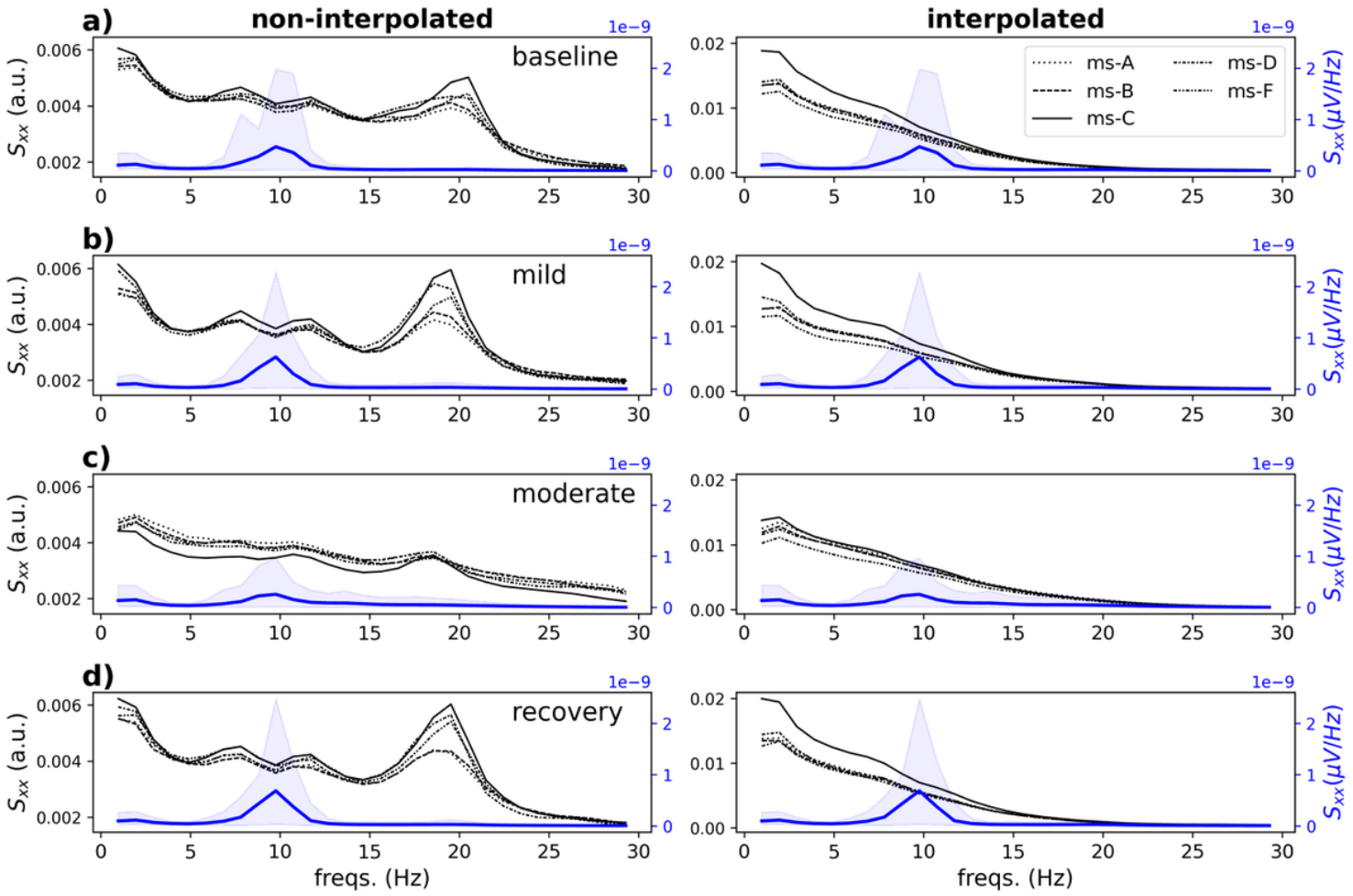

Figure 3

Power spectral densities (PSD, S_{xx}) show 10 Hz oscillations at the EEG sensor level and 20 Hz peaks for characteristic microstate functions for non-interpolated sequences only. *PSD at the EEG sensor level (PSD of the first principal component, mean and 95% confidence interval in blue) and for characteristic microstate functions (mean PSD in black, linestyle indicates the microstate class, see legend on the top right) are shown for each sedation level (a) baseline, b) mild sedation, c) moderate sedation and d) recovery). The EEG-PSD shows a reduced alpha amplitude in moderate propofol sedation. Microstate PSDs show propofol-related attenuation (c) when no interpolation is applied (left).*

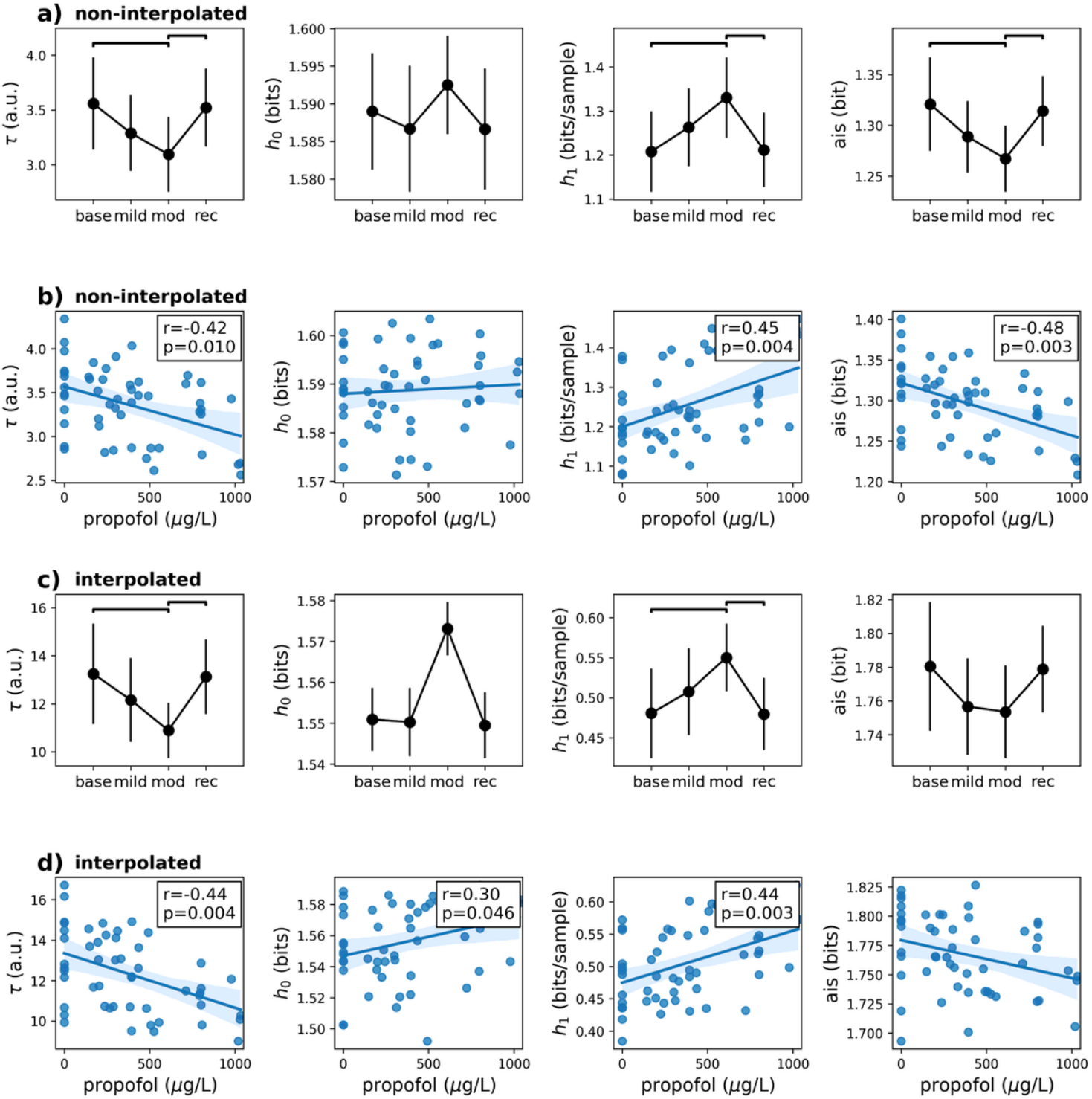

Figure 4

Microstate sequence parameters show faster microstate dynamics and higher entropy rates with increasing propofol sedation. *Transition matrix relaxation time (τ), Shannon entropy (h_0), entropy rate (h_1), and active information storage (AIS) for different sedation levels (a) non-interpolated sequences, c) interpolated sequences), and as a function of propofol plasma concentration (μg/ml) (b) non-interpolated sequences, d) interpolated sequences). Differences at the group level (for the sedation levels base = baseline, mild = mild sedation, mod = moderate sedation, rec = recovery) were assessed with one-way*

ANOVA (α = 0.05) followed by post-hoc pairwise Tukey tests (p_{FWE}<0.05). Significant pairwise differences are indicated by horizontal brackets (a, c). Spearman correlation coefficients are shown as insets in (b, d) if significant (p<0.05).

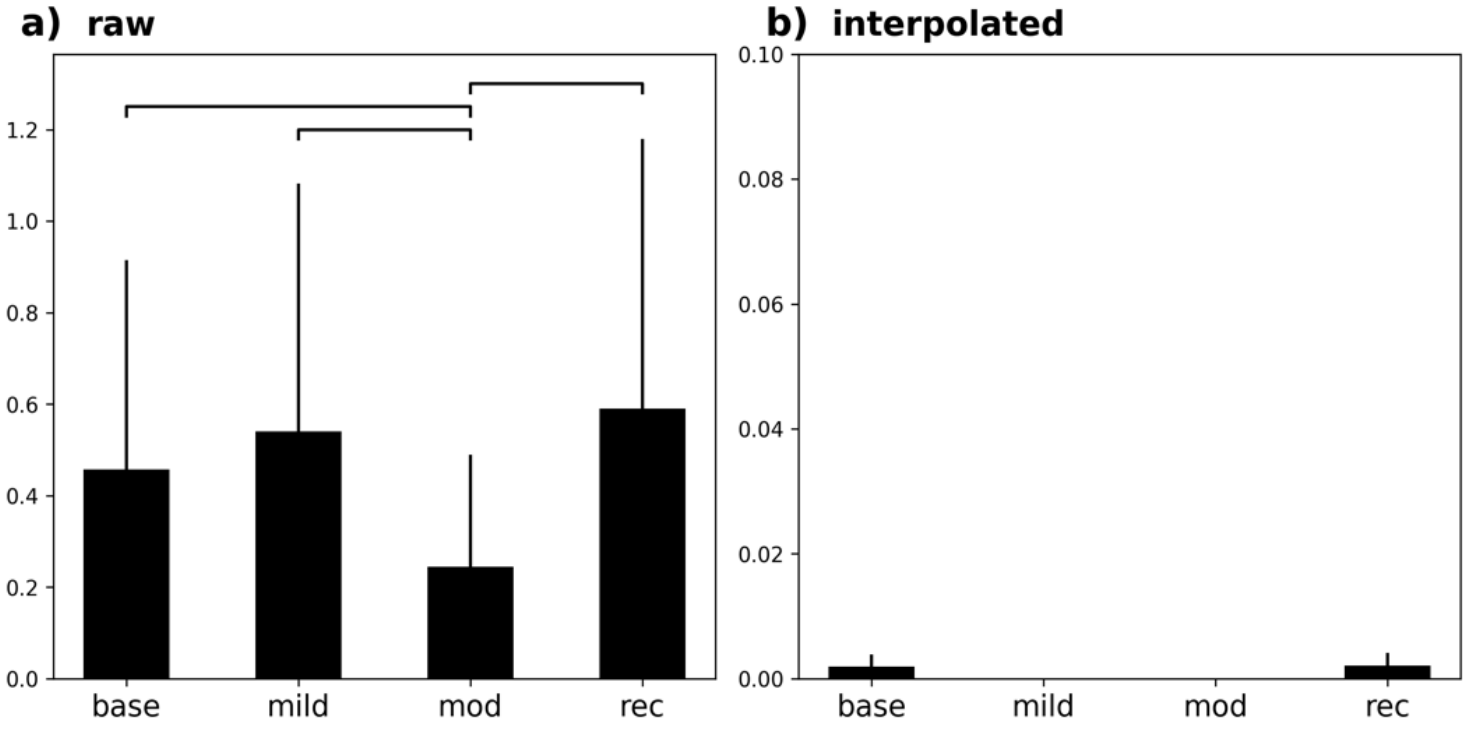

Figure 5

***Temporal irreversibility decreases under moderate sedation for non-interpolated sequences only**.*

Bar graphs indicate the fraction of EEG segments per subject with an asymmetric transition matrix (mean and standard deviation across subjects) in the four sedation levels (base = baseline, mild = mild sedation, mod = moderate sedation and rec = recovery) for a) non-interpolated sequences and b) interpolated sequences. Interpolated sequences show hardly any asymmetric transition matrices and no statistical differences between sedation levels. Note the different y-axis scaling in b) to make differences from zero visible. Differences were tested by one-way ANOVA and post-hoc pairwise Tukey tests. Significant pairwise differences (p_{FWE}<0.05) are indicated by horizontal brackets.

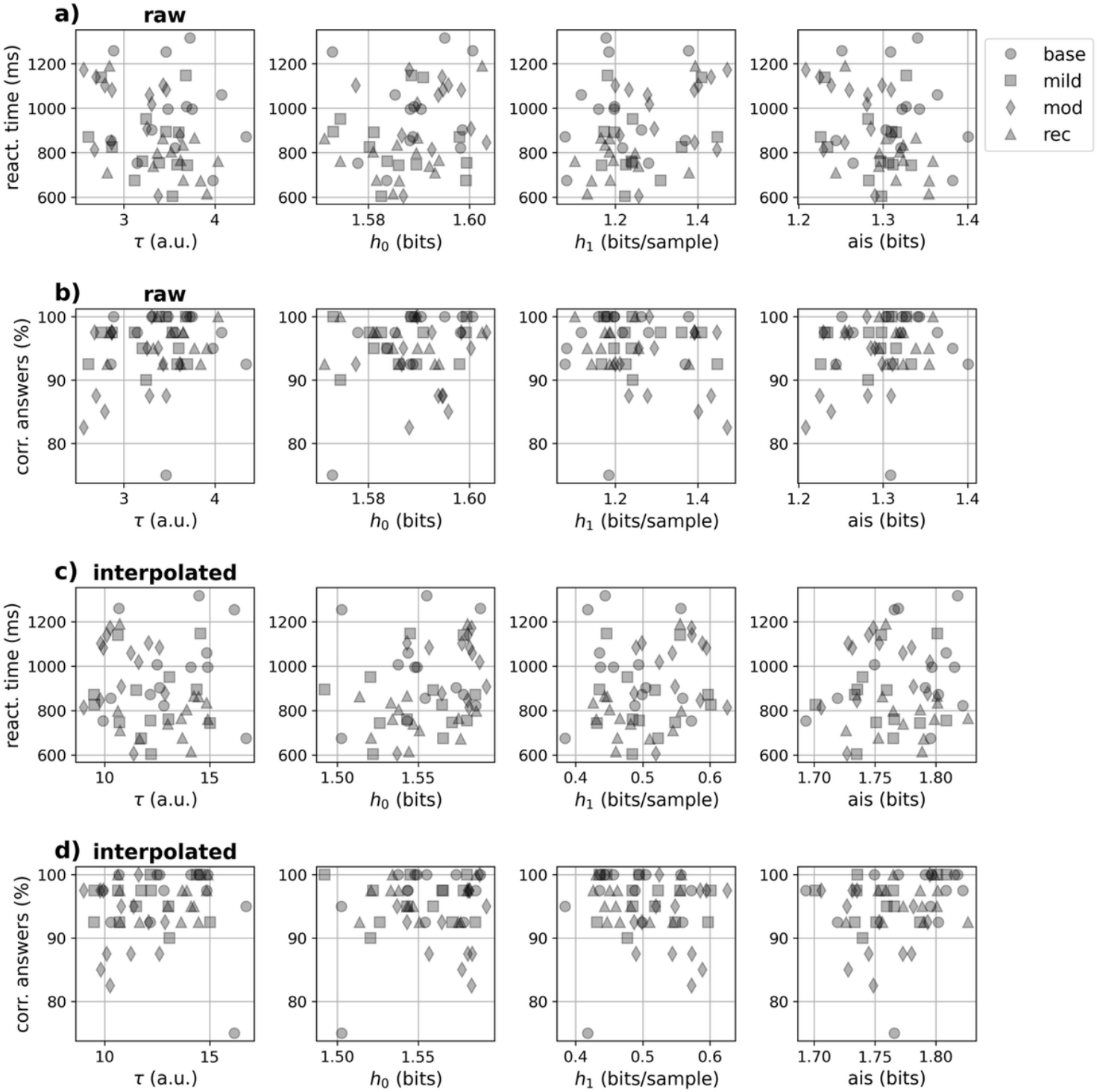

Figure 6

Correlation analysis between microstate sequence parameters and behavioral markers did not reveal any significant results. *Sedation levels are indicated on the upper right (base = baseline, mild = mild sedation, mod = moderate sedation, rec = recovery). a), c) reaction times (ms) and b), d): percentage of correct answer ('hit rates', %) did not show any significant Spearman correlations with the tested microstate sequence parameters (τ, h_0, h_1, AIS) for non-interpolated (a, b) or interpolated (c, d) microstate sequences, respectively. Statistical results were Bonferroni corrected over the n=16 correlation analyses.*